Article

(Terpyridine)copper(II)–Carbon Nanohorns: Metallo-nanocomplexes for Photoinduced Charge Separation

Georgios Rotas, Atula S. D. Sandanayaka, Nikos Tagmatarchis, Toshinari Ichihashi, Masako Yudasaka, Sumio Iijima, and Osamu Ito

J. Am. Chem. Soc., **2008**, 130 (14), 4725-4731 • DOI: 10.1021/ja077090t

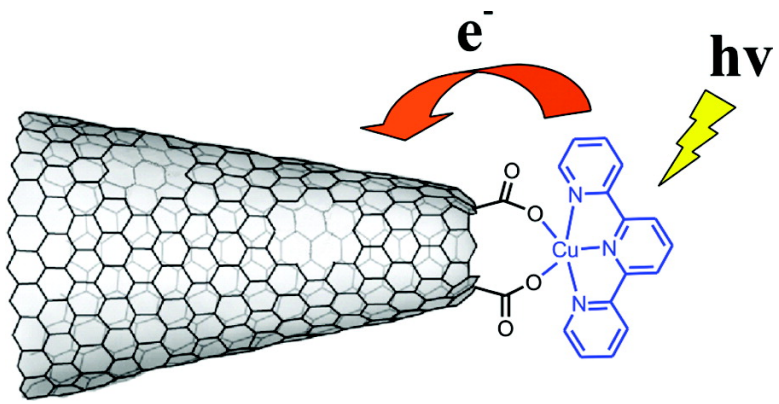

More About This Article

Additional resources and features associated with this article are available within the HTML version:

- Supporting Information
- Links to the 1 articles that cite this article, as of the time of this article download
- Access to high resolution figures
- Links to articles and content related to this article
- Copyright permission to reproduce figures and/or text from this article

View the Full Text HTML

J|A|C|S
ARTICLES
Published on Web 03/18/2008

(Terpyridine)copper(II)−Carbon Nanohorns: Metallo-nanocomplexes for Photoinduced Charge Separation

Georgios Rotas,[†] Atula S. D. Sandanayaka,[‡] Nikos Tagmatarchis,*[,†] Toshinari Ichihashi,[§] Masako Yudasaka,[§] Sumio Iijima,[§] and Osamu Ito*[,‡]

Theoretical and Physical Chemistry Institute, National Hellenic Research Foundation, 48 Vass. Constantinou Ave., Athens 116 35, Greece, Institute of Multidisciplinary Research for Advanced Materials, Tohoku University, Katahira, Aoba-ku, Sendai 980-8577, Japan, and SORST, Japan Science and Technology Agency, NEC Corporation, 34 Miyukigaoka, Tsukuba, Ibaraki 305-8501, Japan

Received September 13, 2007; E-mail: tagmatar@eie.gr; ito@tagen.tohoku.ac.jp

Abstract: New metallo-nanostructured materials of carbon nanohorns (CNHs), within the family of elongated carbon nanotubes, have been prepared by the coordination of copper(II)−2,2′:6′,2″-terpyridine (Cu^{II}tpy) with oxidized carbon nanohorns (CNHs-COOH). The resulted CNHs-COO−Cu^{II}tpy metallo-nanocomplexes have been characterized by diverse analytical spectroscopic tools and cyclic and differential pulse voltammetry. Scanning transmission electron microscopy (STEM), dynamic light scattering (DLS), and energy dispersive X-ray spectroscopy (EDX) measurements have been employed to probe the morphological characteristics and particle-size distribution of CNHs-COO−Cu^{II}tpy as well as to investigate the elemental composition of the metallo-nanocomplex. Steady-state and time-resolved fluorescence emission studies have shown efficient fluorescence quenching, suggesting that electron transfer occurs from the singlet excited state of Cu^{II}tpy to CNHs. Photoexcitation of Cu^{II}tpy resulted in the one-electron reduction of nanohorns with a simultaneous one-electron oxidation of the Cu^{II}tpy unit ($CNHs^{\bullet-}$-COO−$(Cu^{II}tpy)^{\bullet+}$) as revealed by transient absorption measurements. The charge-separated state of $CNHs^{\bullet-}$-COO−$(Cu^{II}tpy)^{\bullet+}$ has been confirmed with the aid of an electron mediator, such as hexyl-viologen dication (HV^{2+}) and an electron−hole shifter in polar solvents.

Introduction

Coordination chemistry of polypyridyl ligands has received considerable attention in recent years and has been continuing active and dynamic.[1] Polypyridylruthenium complexes are well-known for their optical and electronic properties as well as their interaction with DNA.[2] Among polypyridyl ligands, 2,2′:6′,2″-terpyridine (abbreviated as tpy) has been employed in numerous studies, usually binding with metals as a tridentate ligand.[3] Assembly of copper(II)−2,2′:6′,2″-terpyridine (abbreviated as Cu^{II}tpy) with carboxylate ions, accommodating three Cu(II)−N bonds with two *syn*-oriented locations for the carboxylates, has been reported.[4−6] Furthermore, versatile chelation of terpyridine, with other metals beyond copper has been achieved, leading to hierarchically well-defined architectures.[7,8] Moreover, some terpyridine ligands have been covalently attached to [60]-fullerene through either flexible or rigid spacers.[9] Interestingly, however, only a few works have been performed concerning complexation/coordination chemistry of polypyridyl ligands with carbon nanotubes (CNT), i.e. the reported studies concerned direct ligation of Cu^{II}tpy with oxidized CNT[10] and apical coordination between a porphyrin transition metal atom and a pyridyl ligand covalently residing onto the side-walls of CNT.[11]

[†] National Hellenic Research Foundation.
[‡] Tohoku University.
[§] NEC Corp.

(1) (a) Shi, X.; Zhu, G.; Fang, Q.; Wu, G.; Tian, G.; Wang, R.; Zhang, D.; Xue, M.; Qiu, S. *Eur. J. Inorg. Chem.* **2004**, 185. (b) Poleschak, I.; Kern, J.-M.; Sauvage, J.-P. *Chem. Commun.* **2004**, 474. (c) Newkome, G. R.; Cho, T. J.; Moorefield, C. N.; Mohapatra, P. P.; Godinez, L. A. *Chem.—Eur. J.* **2004**, *10*, 1493. (d) Baranoff, E.; Collins, J.-P.; Flamigni, L.; Sauvage, J.-P. *Chem. Soc. Rev.* **2004**, *33*, 147.
(2) (a) Balzani, V.; Juris, A. *Coord. Chem. Rev.* **2001**, *211*, 97. (b) Mihailovic, A.; Vladescu, I.; McCauley, M.; Ly, E.; Williams, M. C.; Spain, E. M.; Nunez, M. E. *Langmuir* **2006**, *22*, 4699.
(3) Hofmeier, H.; Schubert, U. S. *Chem. Soc. Rev.* **2004**, *33*, 373.
(4) (a) Wang, P.; Moorefield, C. N.; Panzer, M.; Newkome, G. R. *Chem. Commun.* **2005**, 465. (b) Wang, P.; Moorefield, C. N.; Panzer, M.; Newkome, G. R. *Chem. Commun.* **2005**, 4405.
(5) Erre, L. S.; Micera, G.; Garribba, E.; Benyei, A. C. *New J. Chem.* **2000**, *24*, 725.
(6) Cano, J.; De Muno, G.; Sanz, J. L.; Ruiz, R.; Lloret, F.; Faus, J.; Julve, M. *J. Chem. Soc., Dalton Trans.* **1997**, 1915.
(7) Rao, C. N. R.; Natarajan, S.; Vaidhyanathan, R. *Angew. Chem., Int. Ed.* **2004**, *43*, 1466.
(8) Newkome, G. R.; Cho, T. J.; Moorefield, C. N.; Cush, R.; Russo, P. R.; Godinez, L. A.; Saunders, M. J.; Mohapatra, P. *Chem.—Eur. J.* **2002**, *8*, 2946.
(9) (a) Armspach, D.; Constable, E. C.; Diederich, F.; Housecroft, C. E.; Nierengarten, J.-F. *Chem. Commun.* **1996**, 2009. (b) Armspach, D.; Constable, E. C.; Diederich, F.; Housecroft, C. E.; Nierengarten, J.-F. *Chem.—Eur. J.* **1998**, *4*, 723. (c) Ku, K. F.; Henbest, K.; Zhang, Y. F. J.; Valentin, S.; Sun, Y.-P. *J. Photochem. Photobiol., A* **2002**, *150*, 143. (d) Zhou, Z.; Sarova, G. H.; Zhang, S.; Ou, Z.; Tat, F. T.; Kadish, K. M.; Echegoyen, L.; Guldi, D. M.; Schuster, D. I.; Wilson, S. R. *Chem.—Eur. J.* **2006**, *12*, 4241.
(10) (a) Wang, P.; Moorefield, C. N.; Li, S.; Hwang, S.-H.; Shreimer, C. D.; Newkome, G. R. *Chem. Commun.* **2006**, 1091. (b) Hwang, S.-H.; Moorefield, C. N.; Dai, L. M.; Newkome, G. R. *Chem. Mater.* **2006**, *18*, 4019.
(11) Alvaro, M.; Atienzar, P.; de la Cruz, P.; Delgado, J. L.; Troiani, V.; Garcia, H.; Langa, F.; Palkar, A.; Echegoyen, L. *J. Am. Chem. Soc.* **2006**, *128*, 6626.

Carbon-based nanostructured materials, such as fullerenes and nanotubes, constitute a unique platform for energy conversion systems, for example, to photovoltaics and optoelectronics.[12] Recently, the combination and integration of carbon nanohorns (CNHs) with photoactive electron donors, such as porphyrins and pyrenes, have started to emerge.[13] The high purity of as-grown metal-free CNHs and the unique morphology in a secondary superstructure forming physically inseparable spherical aggregates[14] are the main characteristics of CNHs, which put them in pole position toward practical technological applications (i.e., photochemical water splitting and reduction of CO_2 to fuels), as compared with the metal and/or amorphous carbon-contaminated carbon nanotube materials.

Herein, the complexation of Cu^{II}tpy as photoexcited electron donor, with carboxylic acids at the opened tips of CNHs (abbreviated as CNHs-COOH), which importantly do not contain any metallic impurities that may potentially affect the photophysical properties, is investigated. The aim of this work is 3-fold, namely, (i) to explore the direct coordination of Cu^{II}-tpy with CNHs-COOH to give CNHs-COO−Cu^{II}tpy, (ii) to assess the characteristics of CNHs-COO−Cu^{II}tpy, and (iii) to evaluate the dynamics of photoinduced intracomplex electron-transfer processes of CNHs-COO−Cu^{II}tpy.

Results and Discussion

Synthesis. The CNHs used in this study were produced by CO_2 laser ablation of graphite in the absence of any metal catalyst under an inert Ar atmosphere (760 Torr) at room temperature.[15] Pristine CNHs were thermally treated under mild oxidative conditions to remove the conical-shaped tip and introduce functional carboxylic units. Then, freshly prepared aqueous Cu^{II}tpy was added in an alkaline solution (NaOH) of CNHs-COOH and the mixture was sonicated for 30 min. After that period, the CNHs-COO−Cu^{II}tpy metallo-nanocomplex was isolated as solid upon filtration through 0.2 μm PTFE membrane filter followed by washing with aqueous $NaPF_6$ and water and dried in vacuum.

Morphological Characterization. Scanning transmission electron microscopy (STEM), energy dispersive X-ray spectroscopy (EDX), and dynamic light scattering (DLS) measurements were used to probe the morphological characteristics and particle-size distribution of CNHs-COO−Cu^{II}tpy, respectively. The secondary spherical superstructure of CNHs is highly retained as demonstrated by STEM (Figure 1a). The average size of the CNHs-COO−Cu^{II}tpy metallo-nanocomplex is around 70 nm. However, it is obvious that further aggregation occurs as a result of the measurement procedures for the STEM imaging, that is, deposition of the CNHs-COO−Cu^{II}tpy metallo-nanocomplex material on the STEM grid. The deposition procedures favor aggregation of the CNHs in larger sizes as evident in the STEM image of Figure 1a, where large aggregates of CNHs-COO−Cu^{II}tpy with a size of 150−180 nm indeed exist. EDX, as a powerful tool for the elemental investigation of carbon-rich nanohybrid materials, verifies the presence of copper and oxygen in the examined CNHs-COO−Cu^{II}tpy metallo-nanocomplex (Figure 1b). Furthermore, the elements of sodium, phosphorus, and fluorine are also identified, thus calling for the presence of some unbound carboxylates units onto the skeleton of CNHs (i.e., in the form of −COONa) as well as partially coordinated Cu^{II}tpy units with PF_6 as the counteranion (cf. Scheme 1; also see Synthesis above and Experimental Section below). Additionally, the EDX map of copper (Figure 1c), corresponding to the STEM image shown in Figure 1a, as well as the line profile of copper of CNHs (Figure 1d) show that the Cu^{II}tpy units are uniformly dispersed on CNHs-COOH. Homogeneous solutions of CNHs-COO−Cu^{II}-tpy metallo-nanocomplex as obtained upon filtration through a micrometer pore-sized membrane filters were used for the DLS measurements. The particle-size distribution of CNHs-COO−Cu^{II}tpy metallo-nanocomplex as estimated by DLS intensity is shown in Figure 1e. In this context, the average diameter of the CNHs-COO−Cu^{II}tpy particle superstructure is around 150 nm (i.e., that is an aggregation of only a couple of CNHs), while metallo-nanocomplexe particles with diameter of 70 nm indeed exist, which is almost same with as-grown CNHs and also agrees with the CNHs size estimated by STEM (Figure 1a).

Characterization. Thermogravimetric analysis of the CNHs-COO−Cu^{II}tpy metallo-nanocomplex allows the quantitative evaluation of tpy ligand complexed with CNHs. In this context, as-grown CNHs show excellent thermal stability up to 800 °C while the oxidized CNHs exhibit a continuous weight loss of about 5% up to 500 °C (i.e., loss of carboxylic units). The CNHs-COO−Cu^{II}tpy metallo-nanocomplex undergoes a weight loss of 17% up to 500 °C due to decomposition of free −COOH as well as loss of tpy (Figure 2).

Spectroscopic insights into the formation of the CNHs-COO−Cu^{II}tpy metallo-nanocomplex are conveyed from Raman and IR spectroscopy. Briefly, in the Raman spectrum of CNHs-COO−Cu^{II}tpy the characteristic D- and G-bands for CNHs were observed at 1279 and 1600 cm^{-1}, respectively (Figure 3).[16] Apparently, after oxidation of CNHs and the introduction of carboxylic units, a number of defect sites are generated onto the skeleton of CNHs as shown from the decrease of the G/D ratio. Moreover, comparison with the Raman spectrum of oxidized CNHs with that after the Cu^{II}tpy complexation revealed that no further significant perturbation on the D- and G-bands occurs. This directly implies that the structural characteristics of oxidized CNHs are kept intact after complexation with Cu^{II}-tpy.

In the attenuated total reflectance-infrared (ATR-IR) spectrum of the oxidized CNHs-COOH, the carbonyl vibration appears as broad shoulder at 1680−1780 cm^{-1}, while vibrations from the C═C bonds derived from the skeleton of CNHs appear in

(12) (a) *Carbon Nanotubes and Related Structures: New Materials for the Twenty-First Century*; Harris, P., Ed.; Cambridge University Press: Cambridge, U.K., 2001. (b) Reich, S.; Thomsen, C.; Maultzsch, J. *Carbon Nanotubes: Basic Concepts and Physical Properties*; VCH: Weinheim, Germany, 2004. (c) *Carbon Nanotubes: Synthesis, Structure, Properties and Applications*; Dresselhaus, M. S., Dresselhaus, G., Avouris, Ph., Eds.; Springer: Berlin, 2001.

(13) (a) Pagona, G.; Sandanayaka, A. S. D.; Araki, Y.; Fan, J.; Tagmatarchis, N.; Yudasaka, M.; Iijima, S.; Ito, O. *J. Phys. Chem B* **2006**, *110*, 20729. (b) Pagona, G.; Sandanayaka, A. S. D.; Araki, Y.; Fan, J.; Tagmatarchis, N.; Charalambidis, G.; Coutsolelos, A. G.; Boitrel, B.; Yudasaka, M.; Iijima, S.; Ito, O. *Adv. Funct. Mater.* **2007**, *17*, 1705. (c) Sandanayaka, A. S. D.; Pagona, G.; Tagmatarchis, N.; Yudasaka, M.; Iijima, S.; Araki, Y.; Ito, O. *J. Mater. Chem.* **2007**, *17*, 2540. (d) Cioffi, C.; Campidelli, S.; Sooambar, C.; Marcaccio, M.; Marcolongo, G.; Meneghetti, M.; Paolucci, D.; Paolucci, F.; Ehli, C.; Rahman, G. M. A.; Sgobba, V.; Guldi, D. M.; Prato, M. *J. Am. Chem. Soc.* **2007**, *129*, 3938.

(14) (a) Iijima, S.; Yudasaka, M.; Yamada, R.; Bandow, S.; Suenega, K.; Kokai, F.; Takahashi, K. *Chem. Phys. Lett.* **1999**, *309*, 165. (b) Kasuya, D.; Yudasaka, M.; Takahashi, K.; Kokai, F.; Iijima, S. *J. Phys. Chem B* **2002**, *106*, 4947.

(15) Pagona, G.; Tagmatarchis, N.; Fan, J.; Yudasaka, M.; Iijima, S. *Chem. Mater.* **2006**, *18*, 3918.

(16) Yamaguchi, T.; Bandow, S.; Iijima, S. *Chem. Phys. Lett.* **2004**, *389*, 181.

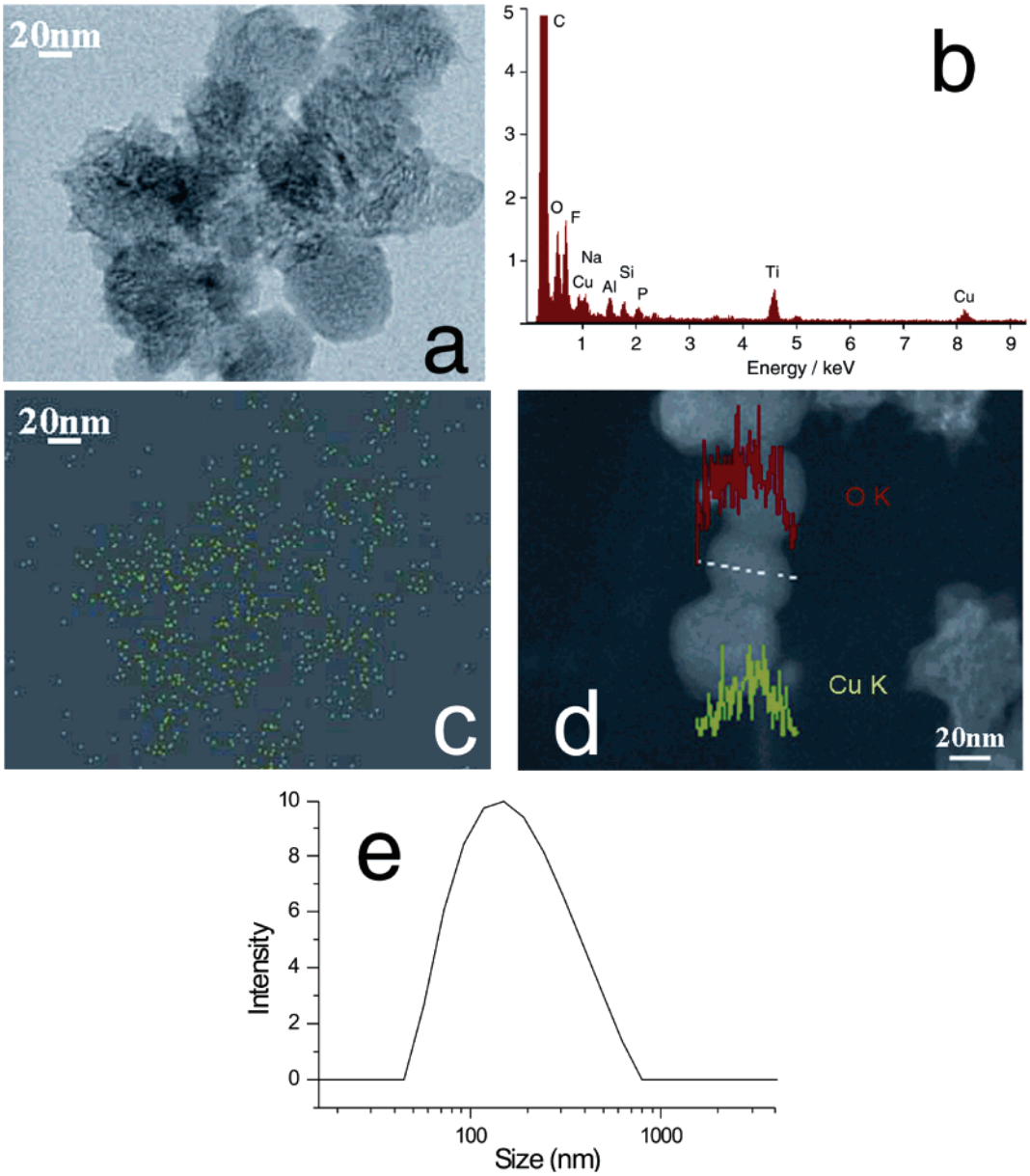

Figure 1. (a) STEM image and (b) X-ray energy dispersive (EDX) spectrum of CNHs-COO−Cu^{II}tpy. The elements of Ti, Al, and Si are detected because of their presence in the microscope equipment, sample holder, and crystal detector. (c) EDX map of copper (green) corresponding to the STEM image, (d) EDX line profile of copper (green) and oxygen (red), and (e) particle size distribution as estimated by DLS intensity of CNHs-COO−Cu^{II}tpyr metallo-nanocomplex.

the region 1460−1600 cm^{-1} and centered at 1555 cm^{-1}.[17] In the case of CNHs-COO−Cu^{II}tpy metallo-nanocomplex, the characteristic C═O peak appears sufficiently depressed at around 1720 cm^{-1} (Figure 4). Additionally, the broad shoulder between 1460 and 1610 cm^{-1} and centered at 1570 cm^{-1} is attributed to C═C units overlapped with the complexed carboxylate moieties.[10a,18] Collectively, the findings based on these ATR-IR measurements suggest the existence of not only complexed carboxylate units onto CNHs but also some free carboxylate units (cf. Scheme 1). The latter result is indicative of a partial complexation of the carboxylates with Cu^{II}tpy, since all of carboxylic units in the superstructure of aggregated CNHs may not be efficiently associated with Cu^{II}tpy due to steric reasons.

In Figure 5 the absorption spectra of free Cu^{II}tpy, CNHs-COOH, and CNHs-COO−Cu^{II}tpy in methanol are compared. Copper(II)−2,2′:6,6′-terpyridine strongly absorbs light at 265−290 nm and 320−340 nm showing sharp bands with fine structures (i.e., 265, 275, 285, 326, and 339 nm). The electronic absorption spectrum of CNHs-COOH does not show any fine structure; however, a continuous absorption from the NIR to the UV−vis region is evident. At first glance, the UV−vis−NIR spectrum of CNHs-COO−Cu^{II}tpy provides unambiguous evidence for the presence of both components of the complex, namely the Cu^{II}tpy and CNHs units. Closer and careful inspection of the spectrum reveals that the characteristic absorption bands of Cu^{II}tpy in the CNHs-COO−Cu^{II}tpy complex are evidently broaden and hardly visible as compared with the free Cu^{II}tpy, although the exact comparison at the same Cu^{II}-tpy concentration is impossible due to the masking effect from

(17) Zhang, M.; Yudasaka, M.; Ajima, M.; Miyawaki, J.; Iijima, S. *AcsNano* **2007**, *1*, 265.
(18) Deacon, G. B.; Phillips, R. J. *Coord. Chem. Rev.* **1980**, *33*, 227.

Scheme 1. Illustrative Structure of the CNHs-COO−Cu^{II}tpy Metallo-nanocomplex

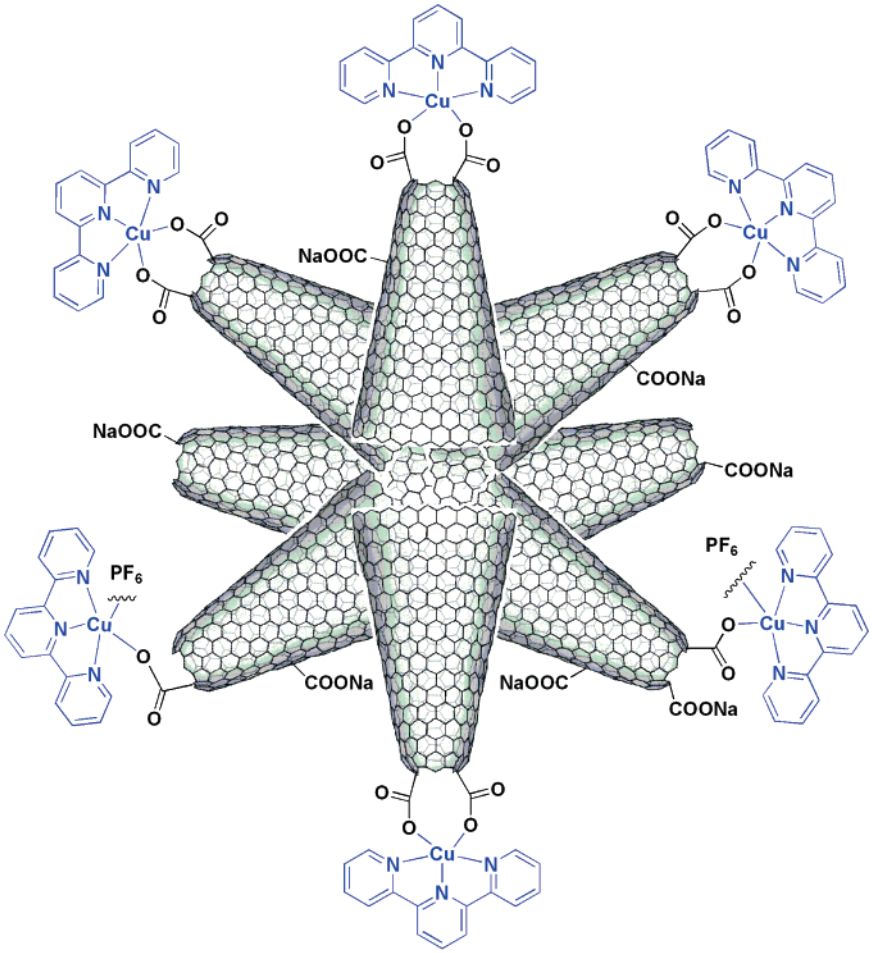

CNHs—see below. This observation is rationalized in terms of the strong absorption of CNHs all throughout the vis region that masks to a great extent the Cu^{II}tpy transitions. Collectively, these observations verify efficient complex formation between Cu^{II}tpy and CNHs-COOH, while furthermore suggest electronic communication between Cu^{II}tpy and CNHs-COOH in the ground states. The latter is in agreement with other reported CNH-based hybrid materials associated with porphyrins, where the broadening of the characteristic Soret and Q bands of the porphyrin moiety is ascribed to electronic communication between the redox-active and photoactive units of the hybrid material.[13]

As reference experiments, when as-grown pristine CNHs as well as hydrogen-terminated CNHs, that is, opened CNHs with reduced oxygen functionalities,[19] were treated with Cu^{II}tpy, no complexation occurred as UV−vis, ATR-IR, and EDX spectra indicate (see Supporting Information, Figures S1−S6). There-

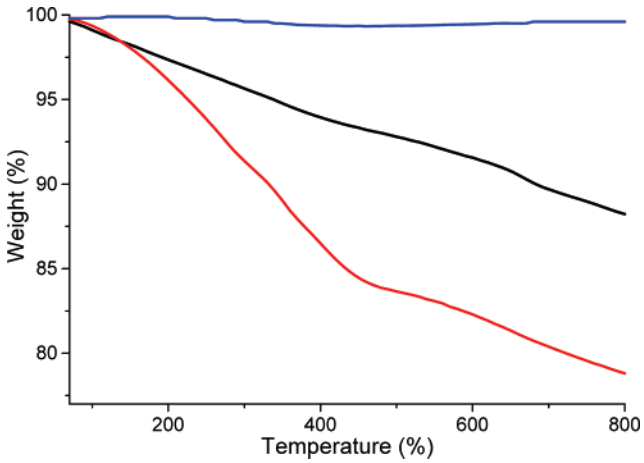

Figure 2. Thermal gravimetric analysis graphs of as-grown CNHs (blue), CNHs-COOH (black) and CNHs-COO−Cu^{II}tpy metallo-nanocomplex (red).

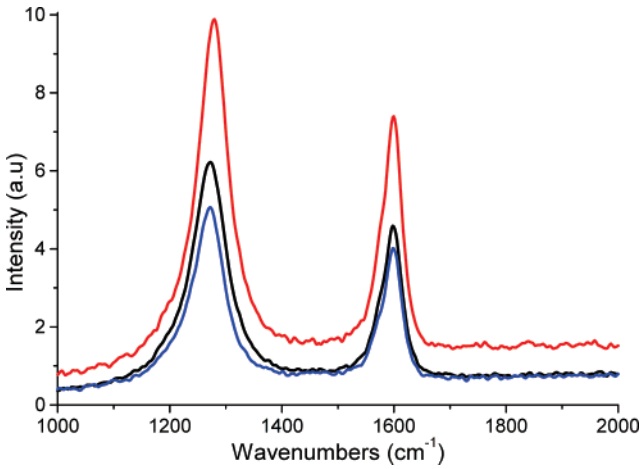

Figure 3. Raman spectra of pristine CNHs (blue) with ratio G/D = 0.79 ± 0.01, oxidized CNHs-COOH (black) with ratio G/D = 0.74 ± 0.01, and CNHs-COO−Cu^{II}tpy metallo-nanocomplex (red) with ratio G/D = 0.74 ± 0.01. Laser light wavelength = 1064 nm, and laser power = 360 mW.

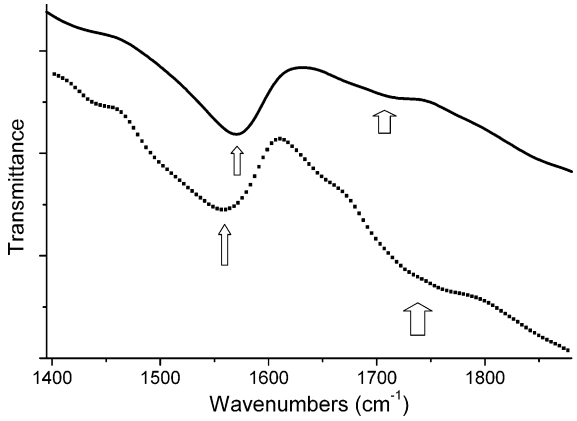

Figure 4. ATR-IR spectra of CNHs-COO−Cu^{II}tpy (solid line) and CNHs-COOH (dotted line).

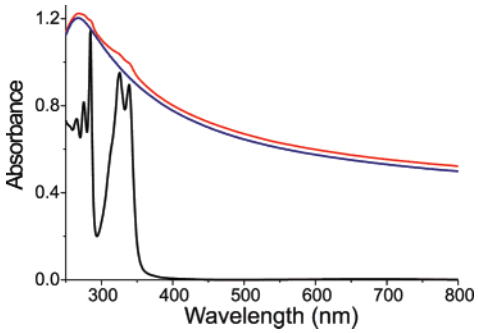

Figure 5. Electronic absorption spectra of free Cu^{II}tpy (black), CNHs-COOH (blue), and CNHs-COO−Cu^{II}tpy metallo-nanocomplex (red), in methanol.

fore, it is concluded that Cu^{II}tpy is recognized and trapped only by the carboxylates present in the CNHs-COOH material.

Treatment of CNHs-COO−Cu^{II}tpy with aqueous NaCN resulted in the disappearance of the characteristic absorptions due to Cu^{II}tpy, indicating that cyanide ions dissociate the Cu^{II}-tpy by liberating tpy ligand absorbing at 285 nm (Supporting Information, Figure S7). At this stage, sufficient evidence on the nature of the new complex derived cannot be provided; however, it is presumed the formation of CNHs-COO−Cu^{II}-$(CN^-)_3$ and tpy. Blank experiments, in which free Cu^{II}tpy samples were treated with NaCN, resulted in an identical UV−vis spectrum with the tpy one. Collectively, these findings indeed confirm that the CNHs-COO−Cu^{II}tpy complexation is controlled by the cyanide ion.

Photophysics and Electrochemistry. The degree of electronic communication in the excited states of the CNHs-COO−Cu^{II}tpy metallo-nanocomplex was assessed by fluorescence spectroscopy. Upon photoexcitation with the 315-nm laser light, the strong fluorescence emission of free tpyCu^{II} appeared at 354 nm with a shoulder at 340 nm. In CNHs-COO−Cu^{II}tpy, however, the fluorescence intensity at 354 nm is significantly depressed with slight increase of the 340 nm peak (Figure 6). Although such a slight increase of the 340 nm peak may be related to the shift of the absorption as seen in Figure 5, the quenching of the main fluorescence peak at 354 nm indicates that adequate association of Cu^{II}tpy with CNHs-COOH allows intracomplex electronic interactions between the Cu^{II}tpy excited singlet-state $^1(Cu^{II}tpy)^*$ and CNHs-COOH.

(19) Miyawaki, J.; Yudasaka, M.; Iijima, S. *J. Phys. Chem. B* **2004**, *108*, 10732.

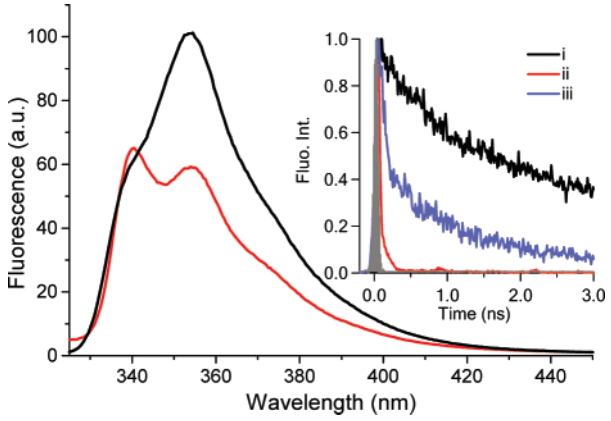

Figure 6. Fluorescence spectra of free Cu^{II}tpy (black) and CNHs-COO−Cu^{II}tpy metallo-nanocomplex (red), observed in MeOH at $\lambda_{exc} = 315$ nm. Inset: Fluorescence decays at 350 nm of (i) free Cu^{II}tpy (in MeOH), (ii) CNHs-COO−Cu^{II}tpy (in MeOH), and (iii) CNHs-COO−Cu^{II}tpy (in THF) at $\lambda_{exc} = 266$ nm from the FHG of a Ti:sapphire laser.

Ensuing the emission quenching of CNHs-COO−Cu^{II}tpy in methanol, fluorescence decay was examined by exciting the second band of the Cu^{II}tpy unit with the 266-nm laser light (inset of Figure 6). The fluorescence decay of free tpyCu^{II} was curve-fitted by the dual-exponential function, from which lifetimes of 850 ps (fraction = 60%) and 4920 ps (fraction = 40%) were evaluated. However, for CNHs-COO−Cu^{II}tpy very short fluorescence emission lifetimes of 60 ps (fraction = 100% in MeOH) and 113 ps (fraction = 65% in THF) were obtained by the curve fitting. The most likely scenario for the excited-state quenching includes charge-separation via $^1(Cu^{II}tpy)^*$. Thus, the rate constants and quantum yields for charge-separation were evaluated to be 1.5×10^{10} s^{-1} (in MeOH) and 8×10^9 s^{-1} (in THF) and 0.93 (in MeOH) and 0.87 (in THF), respectively, from the shorter lifetime components. The slower lifetime with minor fraction (35%) in THF has the same lifetime with free tpyCu^{II}, suggesting the presence of a small amount of unbound Cu^{II}tpy fraction in THF.

The electrochemical properties of CNHs-COO−Cu^{II}tpy were studied by cyclic voltammetry (CV) and differential pulse voltammetry (DPV). The CV measurements were performed on a BAS CV-50 W electrochemical analyzer in deaerated THF−acetonitrile (5:1) solution containing 0.10 M *n*-Bu_4NPF_6 as a supporting electrolyte with the working glassy carbon electrode and the counter Pt electrode. The measured potentials were recorded using an Ag/AgCl (saturated KCl) as reference. From the CV and DPV shown in Figure 7, the oxidation signal of Cu^{II}tpy was observed at 0.47 V vs Ag/AgCl, whereas the reduction peak of CNHs seems to appear at −0.12 V vs Ag/AgCl,[13] as a weak signal as compared with the clearly visible reduction potential of Cu^{II}tpy at −0.73 V vs Ag/AgCl. These observations suggest that a stable radical ion pair includes one-electron oxidation of Cu^{II}tpy, namely $(Cu^{II}tpy)^{\bullet+}$, and one-electron reduction of CNHs, namely $(CNHs^{\bullet-})$, since the energy gap for $CNHs^{\bullet-}$-COO−$(Cu^{II}tpy)^{\bullet+}$, which was calculated as the difference between the oxidation potential of Cu^{II}tpy and the reduction potential of CNHs, is as small as 0.59 eV. Thus, the negative free-energy change for the charge-separated state of CNHs-COO−Cu^{II}tpy via $^1(Cu^{II}tpy)^*$ was evaluated to be ca. −3.0 eV, which confirms the exothermic formation process of $CNHs^{\bullet-}$-COO−$(Cu^{II}tpy)^{\bullet+}$ via $^1(Cu^{II}tpy)^*$.

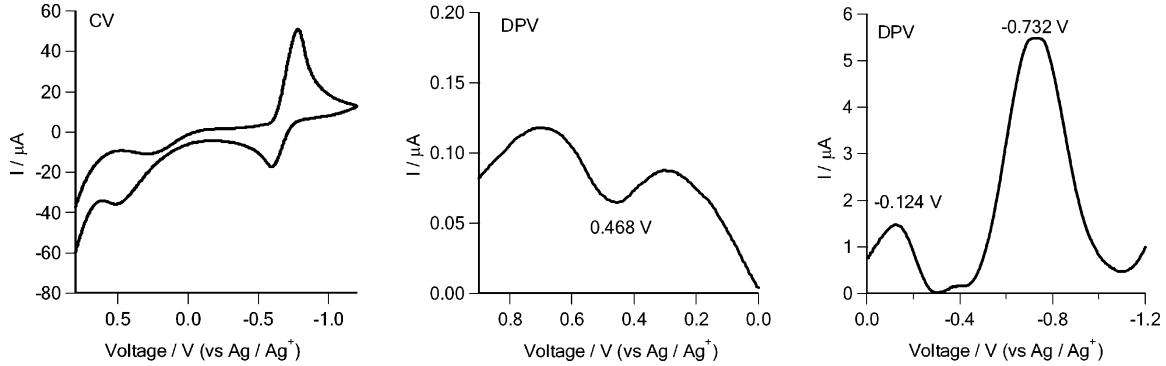

Figure 7. Cyclic voltamogram (CV) and differential pulse voltamograms (DPV) of CNHs-COO−Cu^{II}tpy in deaerated THF−acetonitrile (5:1) solution with a scan rate of 100 mV s^{-1}.

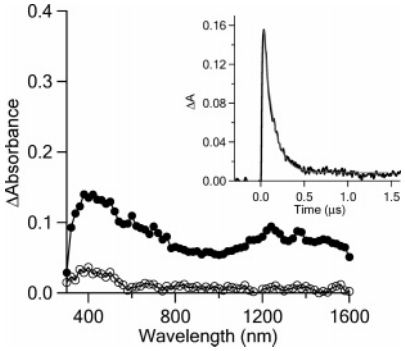

Figure 8. Nanosecond transient absorption spectra of CNHs-COO−Cu^{II}-tpy metallo-nanocomplex observed by 355 nm laser light irradiation (laser power = ca. 3 mJ/pulse, pulse width = 6 ns), at 0.1 μs (●) and 1.0 μs (○) in THF. Inset: Absorption−time profile at 1220 nm.

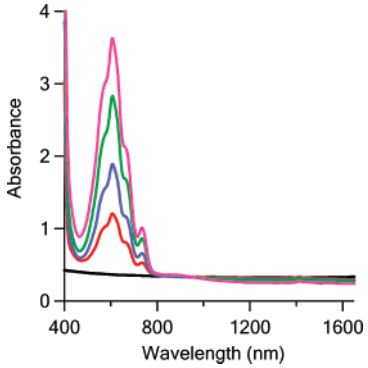

Figure 9. Steady-state absorption spectral changes of CNHs-COO−Cu^{II}-tpy in the presence of 0.5 mM HV^{2+} and BNAH after repeated 355-nm laser light irradiation (ca. 2 mJ/pulse) {[BNAH] = (black) 0, (red) 0.5, (blue) 1.0, (green) 1.5, and (purple) 2.0 mM in deaerated THF}. Repeated time of the 355-nm laser light was set to obtain maximum absorbance for each BNAH concentration.

Complementary transient absorption studies follow the outcome of Cu^{II}tpy fluorescence quenching and the generation of the new photoproducts in CNHs-COO−Cu^{II}tpy. In this context, 355-nm laser light pulses in the nanosecond regime exciting the Cu^{II}tpy unit directed the population of the Cu^{II}tpy singlet exited states. In the transient absorption spectrum of CNHs-COO−Cu^{II}tpy at 0.1 μs (Figure 8), broad bands appeared in the NIR region are attributed to electrons trapped within the reduced nanohorns, namely $CNHs^{\bullet-}$ in line with recent reports;[13] the broad absorption observed in the 400−600 nm region should be indicative of $(Cu^{II}tpy)^{\bullet+}$. Thus, the formation of $CNHs^{\bullet-}$-COO−$(Cu^{II}tpy)^{\bullet+}$ was confirmed as the charge-separated state. Moreover, these transient absorption features are time sensitive; that is, upon the advancing of time after light excitation, the absorbance declines, signifying the charge-recombination development with return of the radical ion pair back to the ground electronic state. Eventually, the rate constants of the charge-recombination process were calculated from the decay (see inset of Figure 8) to be 8.8×10^6 s^{-1} (in THF) and 9.5×10^6 s^{-1} (in MeOH), corresponding to lifetimes for the $CNHs^{\bullet-}$-COO−$(Cu^{II}$-tpy$)^{\bullet+}$ metallo-nanocomplex of 100−110 ns (in THF and MeOH).

Additionally, when 532-nm laser-light was applied to CNHs-COO−Cu^{II}tpy, that predominantly excites the CNH, similar transient absorption bands with the ones acquired by the 355-nm laser were obtained (see Supporting Information, Figure S8), implying the generation of $CNHs^{\bullet-}$ and $(Cu^{II}tpy)^{\bullet+}$ species instantaneously with the nanosecond laser pulse irradiation of π-electron system of CNHs. In this framework, it is reasonable to assume that the electron−hole pair is generated on CNHs moiety at the first step by the direct excitation of the CNHs moiety,[20] in which the hole is captured by the Cu^{II}tpy unit at the second step.

Eventually, to follow the formation of photoinduced charge-separated states within the CNHs-COO−Cu^{II}tpy with 355- and 532-nm laser lights, a set of experiments was conducted upon the addition of an electron mediator and a hole trapping reagents such as hexyl-viologen dication (HV^{2+}) and 1-benzyl-1,4-dihydronicotinamide (BNAH), respectively. All transient species are rapidly quenched, leaving the absorption at 600 nm of $HV^{\bullet+}$ (Supporting Information, Figure S9), as resulted from the mediation of the photogenerated excess electron on $CNHs^{\bullet-}$ to HV^{2+}. In longer time-scale measurements, the $HV^{\bullet+}$ persisted without appreciable decay, suggesting that hole on $(Cu^{II}tpy)^{\bullet+}$ shifts to the sacrificial electron donating BNAH since quick decay of $HV^{\bullet+}$ was observed without BNAH.

Steady-state absorption spectra show accumulation of $HV^{\bullet+}$ (Figure 9) by the repeated laser light irradiation. The maximal absorbance of $HV^{\bullet+}$ acting as electron pool was increased with BNAH concentration, indicating that the back-electron-transfer from $HV^{\bullet+}$ to $(Cu^{II}tpy)^{\bullet+}$ is retarded by transfer the hole to BNAH generating $BNAH^{\bullet+}$, which may irreversibly convert to 1-benzylnicotinamideinum ion (BNA^+). From the maximal absorbance of $HV^{\bullet+}$ the conversion was evaluated to be 50% in THF[21] with 355-nm laser excitation. When the 532-nm laser was employed under the same concentrations with the same laser power (Supporting Information, Figure S10), the conver-

(20) Hasobe, T.; Fukuzumi, S.; Kamat, P. V. *Angew. Chem., Int. Ed.* **2006**, *45*, 755.

sion was slightly lower (i.e., 35%). Since 355-nm laser light excites the Cu^{II}tpy moiety in addition to CNHs, the $HV^{\bullet+}$ generation was the summed result of both the charge separations via $^1(Cu^{II}tpy)^*$ and photoexcited CNHs. On the other hand, since 532-nm laser light excites only CNHs, the $HV^{\bullet+}$ conversion from HV^{2+} was low.

Conclusions

In this study, we were able to expand the utility of metal-free carbon nanohorns toward new photoactive hybrid materials. Carboxylic acid moieties at conical terminals of CNHs were coordinated with Cu^{II}tpy, giving rise to a novel CNHs-COO−Cu^{II}tpy metallo-nanocomplex. The morphology of CNHs-COO−Cu^{II}tpy was investigated with STEM, EDX, and DLS studies, from which the average diameter of the metallo-nanocomplex was evaluated and the presence of metal was confirmed. Steady-state Raman vibration spectroscopy and steady-state electronic absorption and fluorescence emission spectroscopies gave evidence for the formation of CNHs-COO−Cu^{II}tpy, while time-resolved fluorescence and transient absorption measurements demonstrated that photoexcited Cu^{II}tpy serve as an electron donor, resulting in the charge-separated state like as $CNHs^{\bullet-}$-COO−$(Cu^{II}tpy)^{\bullet+}$. Furthermore, direct photoexcitation of the CNHs moiety in CNHs-COO−Cu^{II}tpy also produced the similar radical ion pair. Most importantly, both processes afforded electron-pooling on the viologen in solution, prospective to light-energy conversion systems.

Experimental Section

General Information. All solvents and reagents were purchased from Aldrich and used without further purification unless otherwise stated. All experiments were performed at room temperature unless otherwise stated. Steady-state UV−vis electronic absorption spectra were recorded on a Perkin-Elmer (Lambda 19) UV−vis−NIR spectrophotometer. STEM measurements were carried out using a 002B Topcon operated at an accelerating voltage of 120 kV for imaging. Mid-infrared spectra in the region 550−4000 cm^{-1} were obtained on a Fourier transform IR spectrometer (Equinox 55 from Bruker Optics) equipped with a single reflection diamond ATR accessory (DuraSamp1IR II by SensIR Technologies). The Raman spectra were measured on a Fourier transform instrument (RFS 100 Bruker Optics) employing ca. 360 mW of the Nd:YAG 1064 nm line in a backscattering geometry. The thermogravimetric analysis was performed using a TGA Q500 V20.2 Build 27 instrument by TA in an inert atmosphere of nitrogen. In a typical experiment 1 mg of the material was placed in the sample pan and the temperature was equilibrated at 60 °C. Subsequently, the temperature was increased to 1000 °C with a rate of 10 °C/min and the weight changes were recorded as a function of temperature. Dynamic light scattering measurements were performed in the angular range 20−150° by a ALV/CGS-3 compact goniometer system (ALV GmbH, Germany), using a JDS Uniphase 22 mW He−Ne laser, operating at 632.8 nm, interfaced with a ALV-5000/EPP multi-tau digital correlator with 288 channels and a ALV/LSE-5003 light scattering electronics unit for stepper motor drive and limit switch control. Autocorrelation functions were collected five times at each observation angle for each solution, and they were analyzed by the cumulants method and the CONTIN routine using the software provided by the manufacturers. Hydrodynamic radii were calculated through the Stokes−Einstein relationship. Steady-state emission spectra were recorded with a Fluorolog-3 Jobin Yvon-Spex spectrofluorometer (model GL3-21). The picosecond time-resolved fluorescence spectra were measured using a Ti:sapphire laser (Tsunami) and a streak scope (Hamamatsu Photonics). Nanosecond transient absorption spectra in the visible and NIR regions were measured by means of laser-flash photolysis; 532-nm light from a Nd:YAG laser was used as the exciting source, and Si- and Ge-avalanche-photodiode modules were used for detecting the monitoring light from a pulsed Xe-lamp, as described in our previous reports.[22]

Preparation of CNHs-COOH. Pristine CNHs were thermally treated at 580 °C for 10 min in the presence of oxygen (0.1 MPa) to remove the conical-shaped tip and introduce functional carboxylic units.

Synthesis of Cu^{II}tpy. Terpyridine (3.4 mg) was added to a colorless aqueous solution (5 mL) of copper(II) tetrafluoroborate hydrate (20−22% Cu(II)) (4.6 mg), and the mixture was stirred for 1 h resulting in a blue-green solution.

Synthesis of CNHs-COO−Cu^{II}tpy Metallo-nanocomplex. A suspension of CNHs-COOH (3 mg) in water (10 mL) was sonicated for 15 min resulting in a black solution. Then, 0.25 mL of NaOH (10 N) was added and the mixture was sonicated for 15 min followed by the addition of 0.68 mL of the Cu^{II}tpy solution; the mixture was further sonicated for 1 h. Finally, 0.25 mL of the above NaOH solution was added and the mixture was sonicated for another 30 min. The resulting black precipitate was filtered through a 0.2 μm PTFE filter, washed with water (30 mL), aqueous $NaPF_6$ (0.2M, 5 × 3 mL), water (500 mL), MeOH (30 mL), and Et_2O (30 mL), and dried in vacuo to afford the CNHs-COO−Cu^{II}tpy nanocomplex (3 mg) as a black solid.

Disassembly of CNHs-COO−Cu^{II}tpy Metallo-nanocomplex. A mixture of CNHs-COO−Cu^{II}tpy (1 mg) and NaCN (2 mg) in methanol (5 mL) was sonicated for 30 min. The resulting dark gray solution was examined verifying the disassembly process as described in the text.

Acknowledgment. This work, conducted as part of the award (Functionalization of Carbon Nanotubes Encapsulating Novel Carbon-Based Nanostructured Materials) made under the European Heads of Research Councils and European Science Foundation EURYI (European Young Investigator) Awards scheme, was supported by funds from the Participating Organizations of EURYI and the EC Sixth Framework Program. This work was also supported by a Grants-in-Aid on Scientific Research on Priority Areas (417) from the Ministry of Education, Culture, Sports, Science, and Technology of Japan.

Supporting Information Available: Spectroscopic characterizations and steady-state and transient absorption spectra. This material is available free of charge via the Internet at http://pubs.acs.org

JA077090T

(21) In MeOH, the transient generation of $HV^{\bullet+}$ was confirmed by the transient absorption measurements and also under repeated laser photoirradiation by the eyes; however, the generated $HV^{\bullet+}$ was gradually decreased probably by reaction with MeOH.

(22) (a) Sandanayaka, A. S. D.; Ikeshita, K.; Araki, Y.; Kihara, N.; Furusho, Y.; Takata, T.; Ito, O. *J. Mater. Chem.* **2005**, *15*, 2276. (b) D'Souza, F.; Chitta, R.; Sandanayaka, A. S. D.; Subbaiyan, N. K.; D'Souza, L.; Araki, Y.; Ito, O. *Chem.—Eur. J.* **2007**, *13*, 8277. (c) Chitta, R.; Sandanayaka, A. S. D.; Schumacher, A. L.; D'Souza, L.; Araki, Y.; Ito, O.; D' Souza, F. *J. Phys. Chem. C* **2007**, *111*, 6947.